On the Importance of the MIMO Channel Correlation in Underground Railway Tunnels

Yann Cocheril, Marion Berbineau, Pierre Combeau, Yannis Pousset

On the importance of the MIMO channel correlation in underground railway tunnels

Y. Cocheril, M. Berbineau
INRETS-LEOST, Villeneuve d'Ascq – France
Email: {cocheril, berbineau}@inrets.fr

P. Combeau, Y. Pousset
XLIM/SIC, Poitiers – France
Email: {combeau, pousset}@sic.sp2mi.univ-poitiers.fr

***Abstract*— This paper deals with MIMO channel modeling according to the correlation level in underground railway tunnels for various antenna configurations for the transmitting and receiving arrays. MIMO channel matrices have been computed with a 3D ray-tracing based software at 2.4 GHz and 5.8 GHz in two different tunnel environments: 1) a 1-track empty tunnel with a square cross section, 2) a 1-track tunnel with a square cross section in which a train is parked between the transmitter and the receiver. In this paper, two different strategies are investigated to model the MIMO channel using the Kronecker and the Weichselberger correlation based channel models. The first one is to model the MIMO channel using a single model over the total tunnel length. The second one takes into account the correlation at the receiving side according to the transmitter-receiver distance. In the latter solution, it is possible to isolate specific areas in the tunnel with specific correlation properties and model them in an independent way to take them into account in a system simulation. In this paper, these two modeling strategies are compared in terms of channel capacity.**

***Index Terms*— MIMO channels, correlation, underground tunnels, modal theory, models, Kronecker, Weichselberger**

I. Introduction

New technologies of communication and information are today key components for mass transit systems operation with applications, such as control and command, embedded surveillance, maintenance reporting or video on demand [1]. These wireless systems are often deployed using radiating cables, wave guides, or antennas, using in this case free propagation in tunnels. The wireless systems must be able to maximize data rate (several applications on the same radio medium), or robustness (decreasing the number of radio access points, or increasing the QoS) while avoiding the increase in transmitting power and/or transmission bandwidth.

MIMO (Multiple-Input Multiple-Output) systems appear to answer the needs for robust and high data rate communications, without an additional power or bandwidth consumption [2]. In an environment full of multipaths, the use of multiple antenna arrays at both the transmitting and receiving sides leads to the identification of several independent propagation channels which are linked to the rank of the channel matrix $\mathbf{H}$ [3], [4]. The capacity of the MIMO channel depends on this rank. With spatial correlation or key hole effect in the channel, the $\mathbf{H}$ matrix will be degenerated [5], [6]. Previous works have shown the interest and efficiency of such a system in transport environments [7]. Nevertheless, in a tunnel environment when there is no train, the number of scatters is generally low as well as the spread of the angle of arrival of the rays due to the guided effect. In this context the use of MIMO systems and their efficiency is not obvious [8].

The modal theory [9] shows that in infinite rectangular cross section tunnels, free propagation is possible when the transverse dimensions are large compared to the wavelength. In this specific case, the tunnel can be compared to an oversized lossy waveguide. In this condition, the modal theory shows that only the hybrid modes denoted EH_{mn} are able to propagate, where m and n stand for the mode order. The higher order modes are very numerous near the transmitter, and fade rapidly with the increasing of the distance between the transmitter and the receiver [10]. Far from the transmitter, it remains only two main modes which interfere together. From [10], three areas can be clearly identified: 1) approximately from 0 to 150 m, 2) from 150 to 400 m, 3) above 400 m. According to the decrease of the number of active modes, the full rank of the channel matrix $\mathbf{H}$ can not be guaranteed over all the tunnel length. Subsequently, the ergodic channel capacity C decreases significantly. [8] has shown that confined environments like tunnels lead to narrowband channels at high frequencies. Thus, assuming a time-invariant and flat fading channel, the ergodic channel capacity formulation is [2] :

$$C = \log_2 \left[\det \left(\mathbf{I}_{N_{\mathrm{Rx}}} + \frac{SNR}{N_{\mathrm{Tx}}} \mathbf{H}\mathbf{H}^H \right) \right], \; N_{\mathrm{Tx}} \geq N_{\mathrm{Rx}} \tag{1}$$

Manuscript received December 01, 2008; accepted March 06, 2009; revised March 23, 2009.

This paper is based on "On the importance of an accurate MIMO channel modeling in underground tunnels," by Y. Cocheril, M. Berbineau, P. Combeau, and Y. Pousset, which appeared in the Proceedings of the 2nd International Conference on Wireless Communications in Underground and Confined Areas (ICWCUCA), August 25-27, 2008, Val-d'Or - Québec, Canada.

where N_{Tx} and N_{Rx} are the number of elements at the transmitter and receiver arrays, respectively, $\mathbf{I}$ is the identity matrix, SNR stands for the Signal-to-Noise Ratio, and $\mathbf{HH}^H$ traduces the correlation at the receiving side. Assuming this channel capacity formulation, we have to study the influence of the correlation at the receiver according to the transmitter-receiver distance onto the channel modeling, and thus onto channel capacity.

In this paper, we investigate 4×4 MIMO channel correlation properties for several configurations of the transmitting and receiving arrays, in two underground railway tunnels. A full 3D ray-tracing based wave propagation simulator [11] is used to compute the deterministic channel matrix $\mathbf{H}$ according to the transmitter-receiver distance at 2.4 GHz and 5.8 GHz. In this paper, two channel modeling are proposed. First, the channel is modeled in a global way over all the tunnel length, using the Kronecker [12] and Weichselberger [13] correlation based MIMO models. Then, the tunnel is separated in multiple areas to ensure the stationarity of the correlation properties. In each area, the channel is modeled using the two models. Finally, we present a comparative study between these specific channel models and the simulation results in terms of channel capacity.

This paper is structured as follows. We first introduce in Section II the configurations simulated thanks to a 3D ray-tracing based software. In addition, the Kronecker and Weichselberger models are also described. In Section III, the influence of the geometric configuration of the antennas, in the tunnel and on the trains, on the correlation at the receiver is analyzed. In Section IV, the influence of the channel modeling considering 1) a unique model, or 2) two specific models over two different areas according to the correlation level, is discussed. We will then conclude and give the perspectives to this work.

II. MIMO Channel Simulations

Firstly, we present the two underground railway tunnels, varying the antenna configurations in the tunnel and on the train. Each 4×4 MIMO channel matrix $\mathbf{H}$, obtained for specific antenna configurations in an environment, has been simulated thanks to a 3D ray-tracing based software [11]. This software computes all the possible paths followed by an electromagnetic wave between a receiver and a transmitter, assuming the electromagnetic parameters (relative permittivity, conductivity) of the objects in the scene and a specific number of interactions (reflection and/or diffraction). A previous study has shown that the channel matrix $\mathbf{H}$ can be studied in narrowband [8] for the considered configurations. In this paper, this MIMO channel matrix $\mathbf{H}$ is used to model the channel using existing MIMO channel models such as the Kronecker and the Weichselberger models. These channel models are detailed in a second step.

TABLE I.
Electrical Properties of Materials

	Tunnel	Train
Relative permittivity ε_r	10	2
Conductivity σ (S.m^{-1})	0.01	10^8

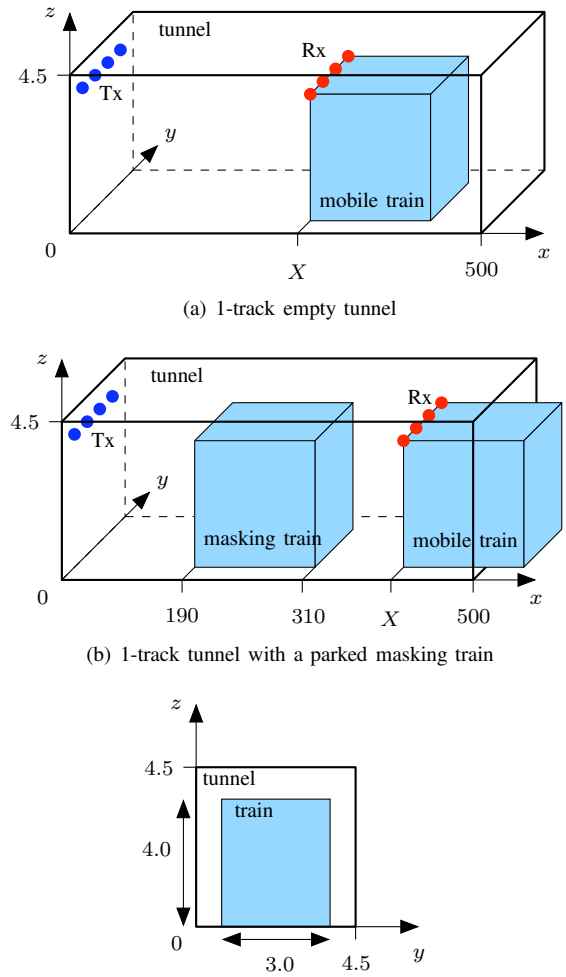

(a) 1-track empty tunnel

(b) 1-track tunnel with a parked masking train

(c) section of the 1-track tunnel

Figure 1. Shapes and dimensions of the underground railway tunnels

A. Description of the tested configurations

Several realistic configurations are simulated, varying the position of the receiver in a tunnel and the orientation of the transmitter and the receiver antennas. The 1-track tunnel (4.5×4.5×500 m) can be 1) empty, or 2) with a parked train (3×4×120 m) between the transmitter and the receiver. Figure 1 illustrates these two configurations. Table I gives the relative permittivity and the conductivity of the materials used to model the environment in the 3D ray-tracing based software. Notice that in the empty tunnel case, this software is configured to compute all the paths which exist between the transmitter and the receiver assuming 10 reflections. On the contrary, the number of reflections is reduced to 9 in the second environment, and the number of diffractions is set to 1. Indeed, many paths can be diffracted by an edge of the parked train.

TABLE II.
4-ELEMENTS POSITIONS (x, y, z) FOR EACH ANTENNAS CONFIGURATION ($i \in \{0, 1, 2, 3\}$)

	x	y	z
TP1	i	0.20	4.30
TP2	0	$\{0.2; 1.2; 2.2; 3.2\}$	4.30
TP3	$0.707\,i$	$0.2 + 0.707\,i$	4.30
RP1	$X + 0.65\,i$	2.25	4.10
RP2	X	$1.275 + 0.65\,i$	4.10
RP3	X	$\{1.6; 1.6; 2.9; 2.9\}$	$\{3.8; 3.15; 3.8; 3.15\}$

Both transmitter and receiver are 4-elements antennas, disposed at various places as indicated in Figure 2. The four elements of the transmitter are 1 m spaced and fixed on the tunnel ceiling. Three configurations are tested (TP1, TP2, TP3): the angle between the orientation of the transmitter axis and the main direction of the tunnel varies from 0 to 90° passing through 45°. The elements of the receiver are closer (0.65 m spaced) due to the lack of space available on the roof of the train. Three configurations are also studied (RP1, RP2, RP3). The two first ones are located on the roof of the train, oriented in the same direction as the longitudinal axis of the tunnel and perpendicular to it, respectively. The third one is located onto the back windshield of the train in a rectangular shape. The coordinates of the elements of each antenna configurations are given in Table II.

Channel matrices $\mathbf{H}$ are computed for all the configurations of the transmitting and receiving arrays 1) over all the tunnel length ($X = [0; 500]$ m) in an empty tunnel, 2) after the end of the parked train ($X = [310; 500]$ m) in the second environment. Indeed, it is not realistic to have the receiver above the parked train in a 1-track tunnel. The sampling rate is equal to 0.5 m.

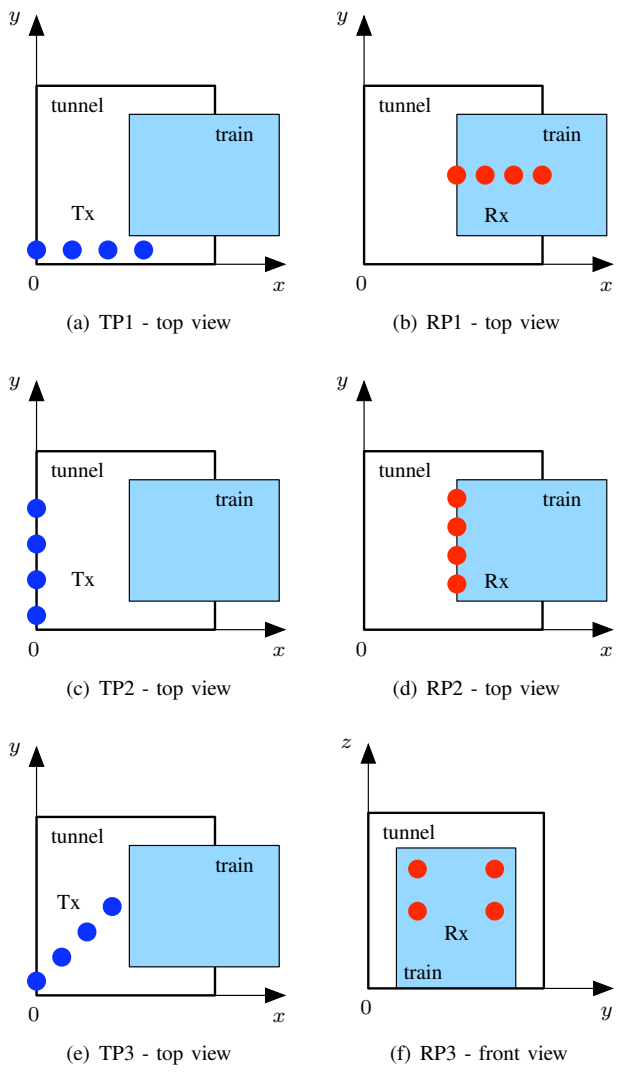

Figure 2. Transmitter (TPx) and Receiver (RPx) antenna configurations

B. Channel modeling

The development and the evaluation of new digital wireless transmission systems need faithful channel models. A lot of models exist in the literature, and they can be classified in two main categories [14].

Physical models are often based on an accurate geometrical description of the propagation environment. They can be deterministic, when they use channel parameters deduced from measurement campaigns or simulation tools (with a 3D ray-tracing based simulator for example) [15]. In this case, the accuracy is high, as the cost in materials, human or computing resources. To eliminate previous drawbacks, researchers have developed many statistical physical models, based on the characterization of the scatters present in the propagation environment [16]. The most used for example are the one-ring and two-ring models [5] and the distributed scatters model [17]. The major drawback of these models remains the determination of the statistical distributions of the scatters in the environment.

Analytical models or stochastic models are independent of the geometric environment description. They are based on the statistical properties of the channel such as the correlation computed from measurements or simulations. There are different possibilities to take into account the correlation between the arrays elements at the receiver and at the transmitter but also in the channel. Several stochastic models were compared in [18]. One of the simplest is the Kronecker model [12] assuming perfect independence of the correlation between transmission and reception sides, while the coupling between the transmitting and receiving arrays can be taken into account using the Weichselberger model [13].

The two models are based on the following decomposition of the channel matrix $\mathbf{H}$, filled with complex coefficients, which can be written as follows:

$$\mathrm{vec}\{\mathbf{H}\} = \mathbf{R}_{\mathrm{H}}^{1/2}\,\mathbf{g} \tag{2}$$

$\mathbf{R}_{\mathrm{H}}$ is the correlation/covariance matrix of the channel, $\mathbf{g}$ is an i.i.d. random fading vector with unit variance and the operator $\mathrm{vec}\{\cdot\}$ stacks a matrix into a vector, columnwise.

1) Kronecker model: The Kronecker model assumes a correlation at the transmitter independent from the correlation at the receiver. So the total correlation of the channel $\mathbf{R}_{\mathrm{H}}$ can be expressed as the Kronecker product ($\otimes$) of the correlation matrices at the transmitter $\mathbf{R}_{\mathrm{Tx}}$ and at the receiver $\mathbf{R}_{\mathrm{Rx}}$:

$$\mathbf{R}_{\mathrm{H}} = \mathbf{R}_{\mathrm{Tx}} \otimes \mathbf{R}_{\mathrm{Rx}} \tag{3}$$

Thus, using (3) in (2), we obtain the following relation for the Kronecker model:

$$\mathbf{H} = \mathbf{R}_{\mathrm{Rx}}^{1/2}\, \mathbf{G}\, \left(\mathbf{R}_{\mathrm{Tx}}^{1/2}\right)^{T} \tag{4}$$

Notice that the covariance matrices can be used instead of the correlation matrices in (4). This formulation is very simple and easily usable once we have obtained the correlation/covariance matrices.

2) Weichselberger model: Contrary to the Kronecker model, the Weichselberger model takes into account the correlation in the channel between the transmitter and the receiver.

Its formulation is based on the well known Singular Value Decomposition (SVD) of the correlation matrices $\mathbf{R}_{\mathrm{Tx}}$ and $\mathbf{R}_{\mathrm{Rx}}$, as:

$$\mathbf{R}_{\mathrm{Tx}} = \mathbf{U}_{\mathrm{Tx}}\, \mathbf{\Lambda}_{\mathrm{Tx}}\, \mathbf{U}_{\mathrm{Tx}}^{H} \tag{5}$$

$$\mathbf{R}_{\mathrm{Rx}} = \mathbf{U}_{\mathrm{Rx}}\, \mathbf{\Lambda}_{\mathrm{Rx}}\, \mathbf{U}_{\mathrm{Rx}}^{H} \tag{6}$$

where:

- $\mathbf{U}_{\mathrm{Tx}}$ and $\mathbf{U}_{\mathrm{Rx}}$ are unitary matrices; their columns contain the eigen vectors of $\mathbf{R}_{\mathrm{Tx}}$ and $\mathbf{R}_{\mathrm{Rx}}$ respectively,
- $\mathbf{\Lambda}_{\mathrm{Tx}}$ and $\mathbf{\Lambda}_{\mathrm{Rx}}$ are diagonal matrices filled with the eigen values of $\mathbf{R}_{\mathrm{Tx}}$ and $\mathbf{R}_{\mathrm{Rx}}$ respectively.

Using (5) and (6) in (4), the following relation can be obtained:

$$\mathbf{H} = \mathbf{U}_{\mathrm{Tx}}\, \left(\mathbf{\Omega} \odot \mathbf{G}\right)\, \mathbf{U}_{\mathrm{Rx}}^{T} \tag{7}$$

where $\odot$ is the Schur-Hadamard product, and $\mathbf{\Omega}$ traduces the coupling between the transmitter and the receiver. Its coefficients $w_{mn} > 0$ are equal to:

$$w_{mn} = \sqrt{E_{\mathrm{H}}\left\{\left|\mathbf{U}_{\mathrm{Rx},m}^{H}\, \mathbf{H}\, \mathbf{U}_{\mathrm{Tx},n}^{*}\right|^{2}\right\}} \tag{8}$$

In (8), $E_{\mathrm{H}}\{\cdot\}$ denotes expectation with respect to $\mathbf{H}$.

III. Channel correlation

In this section, the importance of the orientation of the transmitting and receiving antennas is studied, computing the correlation level at the receiver. The correlation level at the receiver is directly linked with the theoretical channel capacity (1) through the product $\mathbf{H}\mathbf{H}^{H}$. Smaller the correlation level is, greater the theoretical channel capacity is. So, the aim of this section is to identify the best antenna configurations which maximize the channel capacity, and thus offer the maximal diversity which can be traduced into robustness or high data rate capabilities in a wireless communication.

TABLE III.
Average Correlation Coefficient $\bar{\rho}$ in Areas A1, A2 – Empty Tunnel at 2.4 GHz and 5.8 GHz

$f = 2.4$ GHz

	TP1		TP2		TP3	
	A1	A2	A1	A2	A1	A2
RP1	0.83	0.99	0.89	0.98	0.93	0.99
RP2	0.76	0.96	0.50	0.49	0.63	0.59
RP3	0.81	0.97	0.57	0.56	0.59	0.64

$f = 5.8$ GHz

RP1	0.86	0.96	0.79	0.95	0.80	0.94
RP2	0.84	0.88	0.50	0.52	0.51	0.58
RP3	0.79	0.91	0.60	0.54	0.60	0.56

A. Empty tunnel

For each position of the train (from 0 to 500 m), the correlation ρ at the receiver is computed. Figure 3 presents these correlation coefficients according to the distance for all the 9 transmitter-receiver combinations at 2.4 GHz and 5.8 GHz. This figure highlights the increase of the correlation coefficient with the transmitter-receiver distance when the transmitter and/or receiver arrays (TP$j \times$ RP1, TP1 $\times$ RPk, $j, k \in \{1, 2, 3\}$) are oriented in the same direction as the main tunnel axis $\vec{x}$. In these specific cases, two areas can be distinguished. The first one, called A1, starts from 0 to 150 m and shows fluctuations of the correlation level. The second one, named A2, starts from 150 to 500 m and presents high correlation values roughly equal to 1.

On the contrary, the correlation coefficient at the receiver is quite constant over all the tunnel length for specific antenna configurations. The main orientation of these antenna arrays is transverse to the longitudinal axis of the tunnel (TP2 $\times$ RP2 for example). These configurations lead to a smaller coefficient correlation due to the increase of the spatial diversity. The solution, which consists in positioning the antenna arrays onto the back windshield of the train (TP3 $\times$ RPk, $k \in \{2, 3\}$), shows similar performance.

Table III summarizes the correlation coefficients averaged over both areas A1 and A2 identified previously (called $\bar{\rho}$), at 2.4 GHz and 5.8 GHz, respectively. When the angle between the array and the tunnel axis is reduced to $0°$ (TP$j \times$ RP1, TP1 $\times$ RPk, $j, k \in \{1, 2, 3\}$), the mean correlation values are different in each area. In the area A1 (first 150 m), the mean correlation values are between 0.76 and 0.93, while they reached 0.99 in the area A2 (from 150 to 500 m). [19] has explained that spatial diversity can be compared in the tunnel with the concept of modal diversity. Consequently, the correlation between the received modes can increase rapidly with the transmitter-receiver distance, specifically when the transmitting and receiving arrays are oriented along the x axis.

To maximize the modal diversity, the element arrays

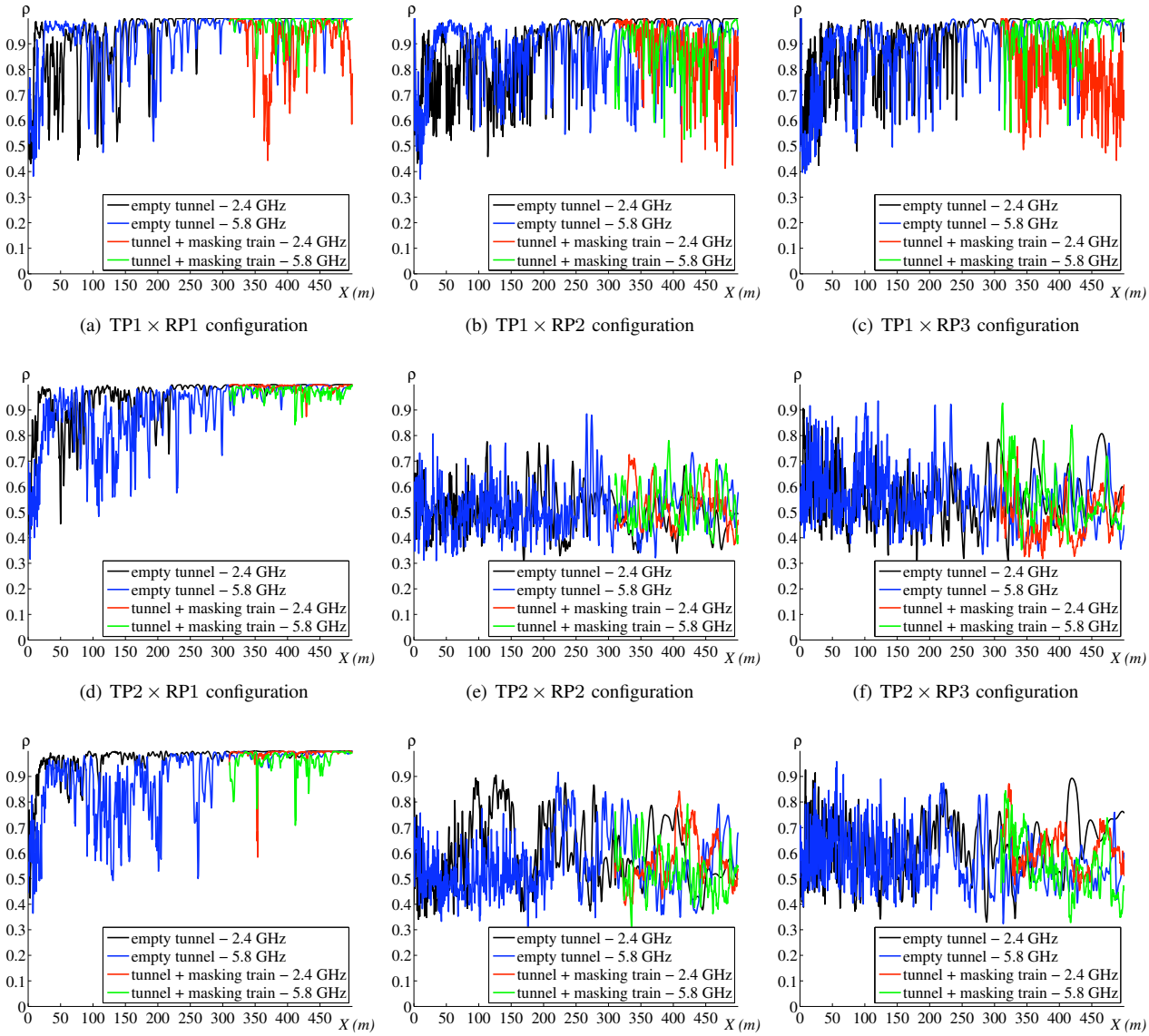

(a) TP1 × RP1 configuration (b) TP1 × RP2 configuration (c) TP1 × RP3 configuration

(d) TP2 × RP1 configuration (e) TP2 × RP2 configuration (f) TP2 × RP3 configuration

(g) TP3 × RP1 configuration (h) TP3 × RP2 configuration (i) TP3 × RP3 configuration

Figure 3. Correlation coefficient ρ at the receiver for all the antenna configurations

have to be oriented in a plane coplanar with the tunnel cross section. Thus, it appears that the correlation level in the TPj × RPk, $j, k \in \{2, 3\}$ configurations decreases significantly ($0.49 < \bar{\rho} < 0.64$ at 2.4 GHz and $0.50 < \bar{\rho} < 0.60$ at 5.8 GHz) and is independent from the transmitter-receiver distance. This small values are possible thanks to the modal diversity which can be maintained in these specific antenna configurations even far from the transmitter [19].

The main observations are the same at 2.4 GHz and 5.8 GHz: 1) two areas A1 and A2 for the configurations TPj × RP1 and TP1 × RPk, $j, k \in \{1, 2, 3\}$, 2) a unique global behavior for the configurations TPj × RPk, $j, k \in \{2, 3\}$. The correlation level is smaller at 5.8 GHz than at 2.4 GHz for the configurations TPj × RP1 and TP1 × RPk, $j, k \in \{1, 2, 3\}$ in the area A2. At this frequency, the modal diversity increases due to a higher number of active hybrid modes that propagate [19].

B. Tunnel with a parked masking train between the transmitting and receiving sides

In the presence of a masking train parked in the middle of the tunnel, the correlation level at the receiver can be computed only between 310 and 500 m. Figure 3 summarizes these results for all the antenna configurations. Only one behavior can be observed: the correlation level varies around a constant mean value from 310 to 500 m. In comparison with the empty tunnel, the correlation level is significantly smaller for the configurations TPj × RPk, $j, k \in \{1, 2, 3\}$ at 2.4 GHz (Table IV). In these specific cases, the parked train added some spatial diversity at the receiver.

C. Conclusion

In this section, two different behaviors of the correlation level have been observed. When the

TABLE IV.
AVERAGE CORRELATION COEFFICIENT $\bar{\rho}$ – TUNNEL WITH A PARKED MASKING TRAIN AT 2.4 GHZ AND 5.8 GHZ

	TP1		TP2		TP3	
f (GHz)	2.4	5.8	2.4	5.8	2.4	5.8
RP1	0.91	0.97	0.99	0.97	0.99	0.96
RP2	0.87	0.89	0.52	0.53	0.57	0.53
RP3	0.80	0.93	0.48	0.55	0.61	0.55

transmitting and receiving antenna arrays are oriented in a plane coplanar with the tunnel cross section, the modal diversity leads to an uncorrelated channel in the overall tunnel length (from 0 to 500 m). On the contrary, two different behaviors can be observed if the antenna arrays at the transmitting and/or receiving sides are oriented along the direction of the longitudinal tunnel axis: close from the transmitter the channel is highly correlated (about 0.90), far from the transmitter it is totally correlated (about 0.99).

IV. CHANNEL MODELING

The previous section has shown that the correlation at the receiver can evolve significantly with the transmitter-receiver distance. This behavior has been only observed in the empty tunnel environment, and particularly when the transmitter and/or receiver are oriented in the longitudinal tunnel direction. This section focuses on the importance to match with real channel behavior in the system performance analysis, computing a channel model over the area A1, and another one over the area A2. The analysis has been performed for the empty tunnel environment. First, we compute a single model over the total tunnel length, using the Kronecker and the Weichselberger models. Then, we compute these two different models over the areas A1 and A2, respectively. Finally, the channel capacity (1) is computed using the two channel models for each areas (A1, A2, and over the total tunnel length) and we compare these results with those obtained directly from the channel matrices computed with the 3D ray-tracing based software in identical area conditions.

Figures 4 and 5 show the channel capacity results using the channel matrices $\mathbf{H}$ obtained respectively from the simulations and the Kronecker model and the Weichselberger model in the TP2 $\times$ RP2 and TP1 $\times$ RP1 configurations, respectively. Notice that these results are averaged over the areas where they are computed (all the tunnel, area A1 or area A2). In the configuration TP2 $\times$ RP2, the antennas are oriented in a plane coplanar with the tunnel cross section. In this case, the previous section has shown that the correlation at the receiver is independent from the transmitter-receiver distance; so the strategy which consists in modeling the channel in two different areas does not seem to be really interesting. Indeed, the channel capacity values are quite similar whatever the strategy we consider. Table V confirms these observations for this specific configuration

TABLE V.
AVERAGE CHANNEL CAPACITY C FOR SNR = 30 dB OVER AREAS A1, A2, AND THE TOTAL TUNNEL LENGTH (A1 + A2) – RESULTS WITH KRONECKER MODEL – EMPTY TUNNEL AT 2.4 GHZ AND 5.8 GHZ

$f = 2.4$ GHz

	TP1		TP2		TP3	
	A1	A2	A1	A2	A1	A2
	A1 + A2		A1 + A2		A1 + A2	
RP1	23.1	14.6	24.4	16.9	25.1	16.8
	18.3		20.2		21.3	
RP2	28.6	20.5	33.8	34.6	32.7	34.5
	25.3		34.6		34.3	
RP3	28.9	19.8	34.6	34.0	34.6	34.0
	25.8		34.4		34.4	

$f = 5.8$ GHz

RP1	24.8	18.0	28.7	20.5	29.0	21.3
	20.7		23.5		24.2	
RP2	30.0	26.1	34.8	33.6	34.5	33.4
	27.9		34.0		33.7	
RP3	30.0	23.9	33.7	34.4	33.6	34.5
	26.7		34.7		34.6	

and for those (TP$j \times$ RPk, $j, k \in \{2, 3\}$) which have highlighted a constant correlation level whatever the transmitter-receiver distance is.

On the contrary the choice of a strategy before modeling the channel is very important in the TP1 $\times$ RP1 configuration. The different values of the correlation level according to the distance lead to a great error onto the mean channel capacity over the total tunnel length. The estimated channel capacity for a SNR = 30 dB is equal to 18.3 $\mathrm{bit.s^{-1}.Hz^{-1}}$. This estimation is far from the mean values obtained in the two areas A1 and A2: 23.1 $\mathrm{bit.s^{-1}.Hz^{-1}}$ and 14.6 $\mathrm{bit.s^{-1}.Hz^{-1}}$ considering the Kronecker model (see Table V), respectively. So, modeling the channel in two different areas appears as a better choice to well model the channel behavior. This observation can be generalized in the other antenna configurations (TP$j \times$ RP1, TP1 $\times$ RPk, $j, k \in \{1, 2, 3\}$) for which a high correlation degree far from the transmitter has been obtained when the transmitter and/or receiver arrays are oriented according to the longitudinal axis of the tunnel.

Moreover, the Kronecker model gives better channel modeling results in terms of channel capacity compared to those obtained directly from the simulations, unlike the Weichselberger one. This observation can be performed in the areas A1 and A2, and also over the total tunnel length. Nevertheless, the Weichselberger model is sometimes better, in some specific configurations, but the differences with the Kronecker model results are too small. So, due to its implementation facility and its great performance, the Kronecker model can be chosen to model the channel in the underground tunnels that we have tested.

Finally, this section has shown that it is useful

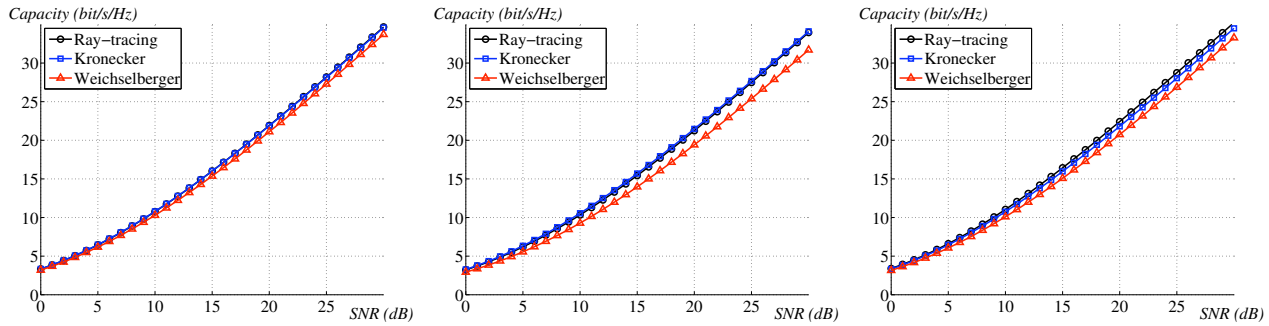

(a) Single channel model from 0 to 500 m (b) Over the area A1 (c) Over the area A2

Figure 4. Average Channel capacities for the simulated channel matrices $\mathbf{H}$ using a ray-tracing based software and both Kronecker and Weichselberger models – TP2 $\times$ RP2 (2.4 GHz)

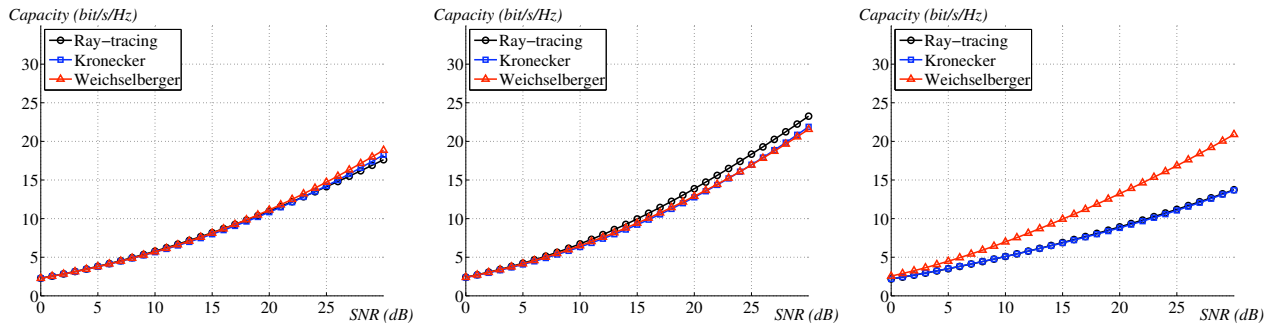

(a) Single channel model from 0 to 500 m (b) Over the area A1 (c) Over the area A2

Figure 5. Average Channel capacities for the simulated channel matrices $\mathbf{H}$ using a ray-tracing based software and both Kronecker and Weichselberger models – TP1 $\times$ RP1 (2.4 GHz)

to identify the different areas in the tunnel where the correlation level varies significantly. With such considerations, an accurate description of the channel capacity in the different areas of the tunnel can be obtained.

V. Conclusion

This paper has presented an interesting study which has focused on the importance to have an accurate description of the correlation variations in an underground tunnel environment, in order to well model the MIMO channel, using Kronecker and Weichselberger correlation based channel models. This study has been performed in two different underground railway environments: 1) a 1-track empty tunnel, and 2) a 1-track tunnel with a masking train parked between the transmitting and receiving sides. In such environment, the 4×4 MIMO channel matrix has been computed thanks to a 3D ray-tracing based software for various antenna configurations at 2.4 GHz and 5.8 GHz.

The study of the correlation level at the receiver has highlighted two different behaviors according to the antenna configurations. When the antennas are oriented in the same direction as the longitudinal axis of the tunnel at the transmitting or receiving sides, the correlation level increases with the transmitter-receiver distance. Thus, two areas have been identified: the first one called A1 starts from 0 to 150 m; the second one named A2 follows the first one until the end of the tunnel (from 150 to 500 m). On the contrary, when the transmitting and receiving antennas are located in a plane coplanar with the tunnel cross section, the correlation is constant over the total tunnel length, due to the diversity of the hybrid modes which propagate. In terms of channel modeling, it is really interesting to subdivide the tunnel in areas where the correlation properties are significantly different, in order to have a better modeling of the channel behavior whatever the transmitter-receiver distance is. When the correlation level is quite constant over the total tunnel length (antennas perpendicular to the tunnel axis), it is sufficient to consider only a single model, valid over the whole tunnel length.

In future works, we will focus on the improvement of the channel modeling results, and on their understanding using the modal theory. More complicated scenes will be also studied (2-track tunnels, stations, etc.), and other antenna configurations will be investigated. Measurements are planned to validate this approach.

Acknowledgment

This work was performed in the framework of the PREDIT research project MOCAMIMODYN (MOdèles de CAnaux MIMO DYNamiques en tunnels pour des applications transport public) in the framework of the I-Trans cluster and the regional CISIT (Campus International Sécurité et Intermodalité des Transports) program. The authors would like to thank the french National Research Agency (ANR), the North Region and

the ERDF (European Regional Development Fund) for financial support.

REFERENCES

[1] M. Berbineau, "Existing or emerging telecommunication systems and their use in guided transports," *Synthèse INRETS*, vol. 40, 2001.

[2] G. J. Foschini and M. J. Gans, "On limits of wireless communications in a fading environment when using multiple antennas," *Wireless Personal Multimedia Communications*, pp. 311–335, June 1998.

[3] R. Gallager, *Elements of information theory*. New York: Wiley, 1968.

[4] Y. M. Berezansky, Z. G. Sheftel, and G. F. Us, *Functional analysis*. Birkhauser Verlag, 1996, vol. 1.

[5] D. S. Shiu, G. J. Foschini, M. J. Gans, and J. M. Kahn, "Fading correlation and its effect on the capacity of multielement antenna systems," *IEEE Trans. Commun.*, vol. 48, no. 3, pp. 502–513, March 2000.

[6] D. Chizhik, G. Foschini, and R. Valenzuela, "Capacity of multi element transmit and received antennas: Correlation and keyholes," *Electron. Lett.*, pp. 1099–1100, 2000.

[7] G. Moniak, M. Berbineau, and J. F. Pardonche, "Robust and high data rate transmissions for security between a bus and a control center," in *VTC '2004-Fall Proceedings*, vol. 2. Los Angeles, USA: IEEE, September 2004, pp. 1377–1381.

[8] Y. Cocheril, P. Combeau, M. Berbineau, and Y. Pousset, "MIMO channel propagation characteristics in tunnels," in *ITST '2007 Proceedings*. Sophia-Antipolis, France: IEEE, June 2007.

[9] K. Laakman and W. Steier, "Waveguides: characteristic modes of hollow rectangular dielectric waveguides," *Appl. Opt.*, vol. 15, no. 5, pp. 1334–1340, May 1976.

[10] M. Lienard, P. Degauque, and J. M. Molina-Garcia-Pardo, "Wave propagation in tunnels in a MIMO context – a theoretical and experimental study," *Comptes Rendus Physique*, vol. 7, no. 7, pp. 726–734, September 2006.

[11] Y. Chartois, Y. Pousset, and R. Vauzelle, "A siso and mimo radio channel characterization with 3d ray tracing propagation model in urban environment," in *ECPS '2005 Proceedings*. Brest, France: IEEE, March 2005.

[12] J. P. Kermoal, L. Schumacher, K. I. Pedersen, P. E. Mogensen, and F. Frederiksen, "A stochastic MIMO radio channel model with experimental validation," *IEEE J. Sel. Areas Commun.*, vol. 20, no. 6, pp. 1211–1226, August 2002.

[13] W. Weichselberger, M. Herdin, H. Ozcelik, and E. Bonek, "A stochastic MIMO channel model with joint correlation of both link ends," *IEEE Trans. Wireless Commun.*, vol. 5, no. 1, pp. 90–100, January 2006.

[14] P. Almers, E. Bonek, A. Burr, *et al.*, "Survey of channel and radio propagation models for wireless mimo systems," *EURASIP Journal on Wireless Communications and Networking*, p. 19 pages, 2007.

[15] L. Schumacher, L. T. Berger, and J. Ramiro-Moreno, "Recent advances in propagation characterisation and multiple antenna processing in the 3GPP framework," in *Proceedings of XXVIth URSI General Assembly*, August 2002.

[16] K. Yu and B. Ottersten, "Models for MIMO propagation channels: a review," *Wireless Communications and Mobile Computing*, vol. 2, pp. 653–666, November 2002.

[17] D. Gesbert, H. Bolcskei, D. Gore, and A. Paulraj, "Outdoor MIMO wireless channels: models and performance prediction," *IEEE Trans. Commun.*, vol. 50, no. 12, pp. 1926–1934, December 2002.

[18] J. Pardonche, M. Berbineau, and C. Seguinot, "Présentation de quelques modèles stochastiques de canal mimo et comparaison expérimentale," *Annales des Télécommunications*, vol. 60, no. 5–6, pp. 649–690, 2005.

[19] J. Molina-Garcia-Pardo, M. Lienard, P. Degauque, D. G. Dudley, and L. Juan-Llacer, "Interpretation of mimo channel characteristics in rectangular tunnels from modal theory," *IEEE Trans. Veh. Technol.*, vol. 57, no. 3, pp. 1974–1979, 2008.

Yann Cocheril was born in Rochefort, France, on March 30, 1980. He received his PhD degree in information technology and communication sciences from the University of Poitiers in 2006, and his MS and BS degrees in electrical and information engineering from the University of Poitiers in 2002 and 2001, respectively.

He is currently a postdoctoral researcher at the french national institute for transport and security research (INRETS). His current research interests include the SISO and MIMO channel modeling in underground tunnels and the optimization of the physical layer in such confined environments, for robust and high data rate transmissions in railway applications.

Marion Berbineau was born in Toulouse, France, on September 18, 1962. She received the Engineer degree in electronics, automatic and metrology from Polytech'Lille (France) and the PhD in electronics from the University of Lille respectively in 1986 and 1989.

She joined INRETS as a full time researcher in telecommunications in 1989. She is currently Research Director and Director of the LEOST laboratory.

Dr Berbineau field of expertise are EM propagation, channel characterization and modeling for transport environments, signal processing for wireless communication systems, MIMO systems. She is involved in several national and European projects. She is author and co-author of several publications and patents. Dr Berbineau is an IEEE member, affiliated to the VTS society.

Pierre Combeau was born in Angoulême, France, on June 12, 1978. He received the M.S. degree in mobile radio-communications and image processing and the Ph.D. degree in signal processing and telecommunications from the University of Poitiers, respectively in 2001 and 2004.

Since 2005, he is professor assistant at the University of Poitiers in the department SIC (Signal Image Communications) of the Xlim Laboratory. His fields of expertise include the study of the electromagnetic waves propagation for the SISO and MIMO wireless communication systems.

Yannis Pousset received the Ph.D. degree in mobile radiocommunication from the University of Poitiers, in 1998.

Since 2000, he is professor assistant at the University of Poitiers in the department of electrical engineering. He develops its research activities in the SIC-XLIM (Signal Image and Communication) laboratory of the University of Poitiers. His research interests include the study of the electromagnetic waves propagation for the SISO and MIMO wireless communication systems.